Acta of Bioengineering and Biomechanics
Vol. 18, No. 2, 2016

Original paper
DOI: 10.5277/ABB-00406-2015-02

Biomechanical and fluid flowing characteristics of intervertebral disc of lumbar spine predicted by poroelastic finite element method

LI-XIN GUO[1]*, RUI LI[1], MING ZHANG[2]

[1] School of Mechanical Engineering and Automation, Northeastern University, Shenyang, 110819, China.
[2] Interdisciplinary Division of Biomedical Engineering, The Hong Kong Polytechnic University, Hong Kong, China.

Purpose: This study is to reveal the deformation of intervertebral disc (IVD), the stress distribution of solid phase and liquid phase, the variation of fluid flux and flow velocity in lumbar spine and the influence of different permeability parameters on them under intermittent compressive loading. *Methods*: A poroelastic FEM of L4-L5 is assigned with different permeability parameters to analyze the deformation, stress distribution and fluid convection under intermittent compressive loads. *Results*: The results show that the pore pressure of IVD decreases with time, but the effective stress increases under intermittent compressive loads. The axial and radial strain will increase and fluid loss will recover at a more rapid rate if the permeability of endplate increases during unloading period. The velocity vectors show that most of the liquid in the disc flows into vertebrae through endplates and only a small quantity of liquid flows through the annulus fibrosus at the loading step, however, at the unloading step, almost all the liquid flowing into IVD is through the endplates. *Conclusions*: The changing rate of pore pressure and effective stresses of nucleus pulposus and annulus fibrosus with higher permeability is smaller than that with smaller permeability. The degenerated endplate (with low permeability) yields high flow velocity decreasing gradient, which might impede liquid inflowing/outflowing smoothly through the endplates. The fluid flowing velocity in loading phase is faster than that in unloading phase, so a short resting time can relieve fatigue, but could not recover to the original liquid condition in IVDs.

Key words: *lumbar spine, poroelastic finite element model, permeability of cartilage endplate, intermittent compressive load*

1. Introduction

Low back pain is a major health problem that has an enormous impact on many people during their working years, it has become an important cause of disability, and investigations on biomechanical characteristics of the lumbar spine and etiology of IVD diseases have attracted much more attention [12], [13], [15], [19]. Wilke et al. [29] carried out in vivo experiments for daily work and activity and measured the IVD pressure of human lumbar spine. van der Veen et al. [28] tested the in vitro validity of flow-related mechanics of IVD to investigate whether the liquid can flow back into the disc during unloading periods. Przybyla et al. [22] studied the effect of destruction of annulus fibrosus and endplates on the stress distribution related with IVD degeneration. Smith et al. [23] discussed the effect of annulus fibrosus on the biomechanical properties of normal and degenerative IVDs.

Many in vitro experiments have been carried out to study mechanical characteristics of the spine. Some in vitro experiments indicated that, though the specimens were kept moist, the measured results of fluid outflow existing in loading stage did not match the results of fluid inflow in unloading stage [28]. This difference not only changed the reaction of motion segments during recovery period, but also changed the mechanical behavior of the whole motion segment in subsequent loading periods. The influence accumulation in experiments will lead to further differences compared with actual results [20].

As it is difficult to obtain all-around biomechanical characteristics of the spine only from experimen-

* Corresponding author: E-mail: lxguo@mail.neu.edu.cn
Received: June 21st, 2015
Accepted for publication: September 17th, 2015

tal measurements, finite element methods have been widely used to study various biomechanical characteristics of human spine. Finite element analysis and experimental research may complement each other, which can help us to fully understand the physiological characteristics of the spine, and prevent and cure the low back pain and spine diseases [25], [12], [13]. Due to the complexity of human spine system, especially the poroelastic characteristics, poroelastic FEMs have been widely used in current research, which are established based on the solid consolidation theory and can mimic the interaction between solid phase and liquid phase in porous media. Poroelastic principle implies that IVD tissue structure consists of two parts, the incompressible solid phase with porosity and the incompressible liquid phase flowing across the solid phase porosity.

Wu and Chen [30] firstly analyzed the behavior of spine using a three-dimensional FEM with poroelastic property. Cheung et al. [7] studied biomechanical responses of IVDs under static and vibration loading, and their results showed that the fluid flow in the spine was due to internal gradient pressures caused by external loading effect. Natarajan et al. [20] and Chagnon et al. [6] established the healthy and degenerated poroelastic FEMs to analyze the mechanical performance of degenerative IVDs, respectively. Natarajan et al. [20] developed a nonlinear poroelastic FEM to predict the failure process of IVD under physiological relevant cyclic loading. Schmidt et al. [26] established a nonlinear poroelastic FEM to study the physiological reaction of spine under the daily dynamic physiological activities. Schmidt et al. [26] predicted the temporal shear response under various shear loads using a poroelastic FEM, and the effects of nucleotomy and facetectomy as well as changes in the posture and facet gap distance, were analyzed as well. Gohari et al. [10] developed a nonlinear poroelastic FEM of intervertbral disc, in which the viscoelastic Euler beam element and rigid link element were used to create the disc and vertebra, respectively, and the prolonged loading and cyclic loading were applied to the models to check the computation efficiency.

Investigations show that the permeability of endplate plays an important role in degeneration progress of IVD [24]. However, in many poroelastic studies, the permeability of endplate was usually set with a single value, in which the degenerative IVD did not consider the endplate degeneration and influence of its permeability on fluid flow during loading and unloading periods. These simplifications are not helpful for understanding the detailed biomechanical behavior of IVD [20]. Therefore, in this study, a poroelastic FEM of lumbar spine was developed and the permeability parameters of endplates were set with different values to examine the influence of different permeability on biomechanical characteristics of IVD under actual loading conditions.

2. Materials and methods

Finite element method can apply the spinal structure with complicated material property and simulate various complicated loading effects [5], [21]. In this study, the representative lumbar spine L4-L5 segment [7] is adopted. The software ABAQUS is used to establish a three-dimensional poroelastic FEM of L4-L5 disc-vertebra segment. To examine the influence of different permeability on biomechanical characteristics of IVD under actual loading conditions, material parameters of endplates are assigned with three permeability parameters.

2.1. Modeling

According to the main research purpose, only the L4 and L5 vertebral bodies, cartilage endplates and IVD are established, ignoring posterior elements, joint capsule and ligaments. The geometric structure of L4-L5 FEM is based on our previous experiment data [12], [13] and other literature [9], [2]. The annulus fibrosus of IVD is simplified as a structure with cross-link fibers embedded in annulus ground substance, which occupied 19% of the annulus volume [17]. The vertebral bodies, nucleus pulpous, endplates and annulus ground substance are modeled with the 20-node reduced integral quadratic element C3D20RP.

2.2. Material property

Due to the fluid flowing mainly through nucleus pulpous, annulus fibrosus, cartilage endplates and cancellous bones, these components are assigned with poroelastic material property. The material properties are listed in Table 1, which are obtained from the literature [3], [11], [16], [25], [20], [24]. The material parameters of poroelastic mechanical formula consist of the drained Young's modulus E, Poisson's ratio v, porosity n, and permeability k. As the permeability ratio k in tissues and the porosity n reduce gradually

Table 1. Material properties of L4/L5 motion segment for healthy and degenerated discs

Components	Drained Young's modulus E (MPa)	Poisson's ratio γ	Initial void ratio e_0	Initial permeability k_0
Nucleus	1.5[a]	0.1[a]	4.0[a]	0.3 e-15 m^4/Ns[a]
Annulus	2.5[a]	0.1[a]	2.33[a]	0.11 e-15 m^4/Ns[b]
Endplate	20[e]	0.1[a]	4.0[a]	*
Cancellous bone	100[c]	0.2[a]	0.4[a]	100 e-15 m^4/Ns[a]
Cortical bone	12,000[c]	0.3[c]	-	-
Fibers	500[d]	0.3[d]	-	-

Note: [a] Argoubi and Shirazi-Adl [3]; [b] Gu et al. [11]; [c] Natarajan et al. [20]; [d] Lee and Teo [16]; * The permeability of endplate: 1.0 e-13 m^4/Ns, 7.0 e-15 m^4/Ns (Shirazi-Adl and Parnianpour [25]), 1.0 e-48 m^4/Ns (Schroeder et al. [24]).

with the increase of compressive strain, the reduced permeability k can be expressed as follows

$$k = k_0\left[\frac{e(1+e_0)}{e_0(1+e)}\right]^2 \exp\left[M\left(\frac{1+e}{1+e_0}-1\right)\right], \quad e=\frac{n}{1-n}.$$

In the saturated case, the void ratio e is the ratio of fluid volume to porous solid volume, e_0 and k_0 are initial void ratio and initial permeability, respectively. For simplification, a uniform pore distribution is assumed to nucleus pulpous and annulus fibrosus. According to the poroelastic theory, the total stress acting on a point is assumed to be made up of a pore pressure on liquid phase and an effective stress tensor on solid phase. At the initial time, the fluid levels in nucleus pulposus and annulus fibrosus are 80% and 70%, respectively [6].

2.3. Boundary and loading conditions

Only the compressive load was imposed, so the boundary conditions were set as (1) restricting all the degrees of freedom of L5 bottom surface and (2) imposing a constant pore pressure of 0.25 MPa on external surfaces of the mode to mimic interior pressure of human body [26], [27].

The intermittent compressive load imposed on the model represents one half-day working condition. The working period is 4 hours and every hour working time has 10 minute resting time. During the resting time, a physiological compressive force of 350 N [26] is imposed on the model. During the working time, an axial compressive force of 1000 N represents common labor intensity, such as standing work or lifting lightweight items in hands, to mimic the compressive load on lumbar spine [20]. In order to keep the swelling pressure balance, a 500 N preload is imposed on the model at first.

The fluid flowing through endplates might be blocked by blood clotting, therefore one needs to create a block effect in simulations [4], [18]. There is a resistance between the contact surface of vertebral body and IVD, which is called as blocking phenomenon of endplates. In order to compare the effect of endplate permeability, different permeability parameters of cartilage endplate are set as 1.0e-13 m^4/Ns, 7.0e-15 m^4/Ns and 1.0e-48 m^4/Ns, respectively.

3. Results

3.1. Model validation

In order to verify the validation, an axial compressive load of 1000 N (no intermittent) is applied to the model for four hours and the results show that the axial displacement is 1.51 mm. Adams et al. [1] reported that a 1000 N compressive load for 6 hours yielded the axial displacement of 1.53 mm; Ferguson et al. [8] applied a 800 N compressive load for 16 hours and the axial displacement was 1.6 mm; Argoubi and Shirazi-Adl [3] imposed a 400 N compressive load with boundary pressure of 0.1 MPa for 2 hours and the axial displacement was 0.7 mm. Comparing with these experiment and simulation results, it can be proved that the model established in this study is reasonable.

3.2. Daily activity

After 4 hours intermittent compressive loading (with 10 minute resting for every hour), the height of IVD reduced by 1.48 mm, 1.33 mm and 1.16 mm, respectively, corresponding to 3 different permeability parameters of endplates (1.0e-13 m^4/Ns, 7.0e-15 m^4/Ns and 1.0e-48 m^4/Ns) in Fig. 1.

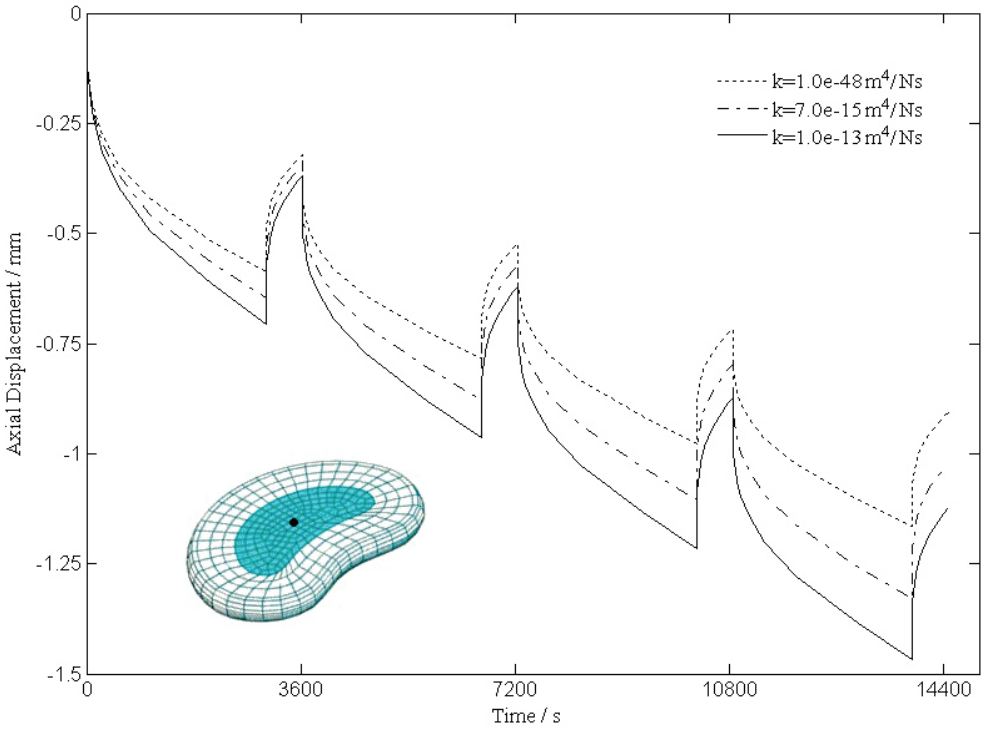

Fig. 1. Prediction of disc height reduction of L4-L5 disc-vertebra segment
(the initial permeability of k = 1.0 e-13 m^4/Ns, k = 7.0 e-15 m^4/Ns, k = 1.0 e-48 m^4/Ns, respectively)

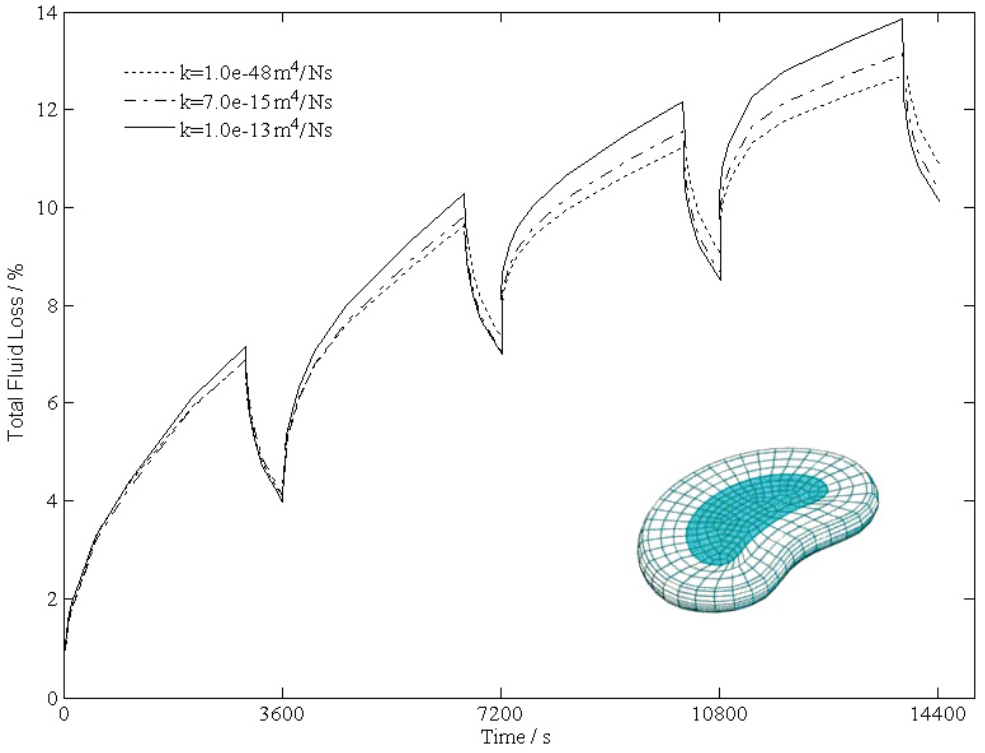

Fig. 2. Total disc fluid loss of the disc
(the initial permeability of k = 1.0 e-13 m^4/Ns, k = 7.0 e-15 m^4/Ns, k = 1.0 e-48 m^4/Ns, respectively)

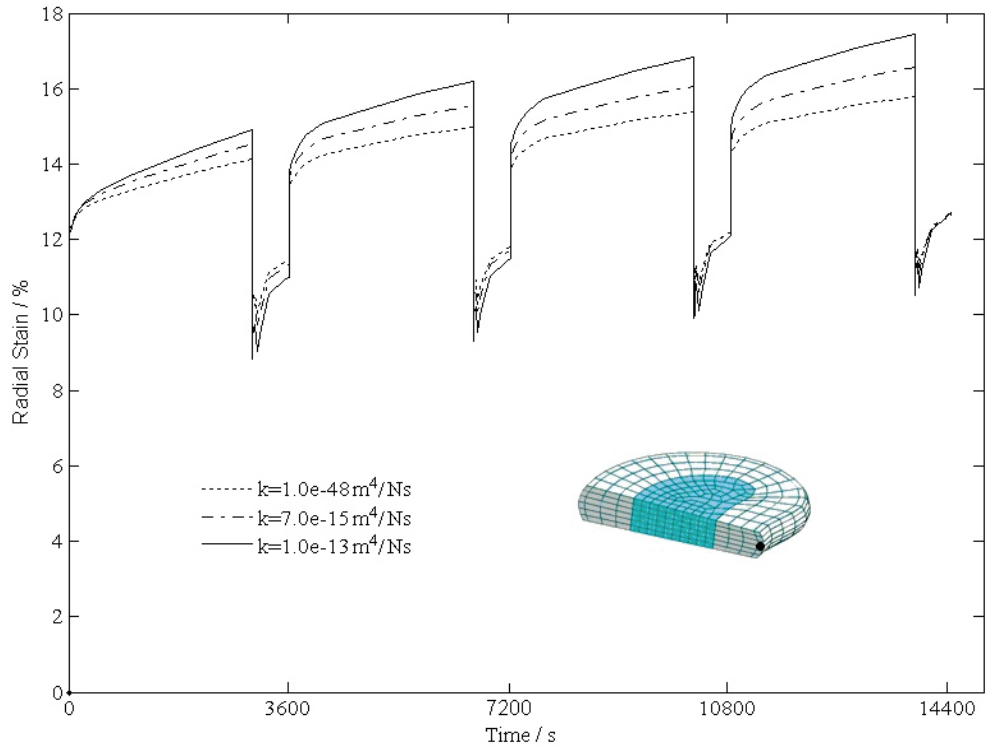

Fig. 3. Radial tensile strains in the posterior region of annulus
(the initial permeability of k = 1.0 e-13 m^4/Ns, k = 7.0 e-15 m^4/Ns, k = 1.0 e-48 m^4/Ns, respectively)

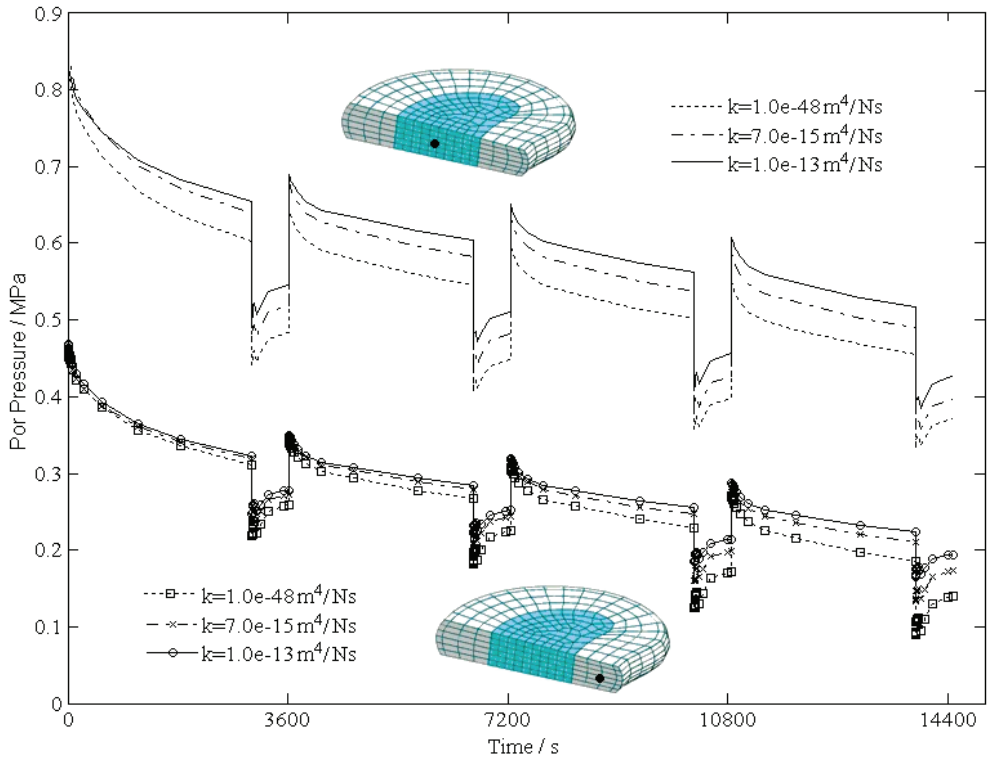

Fig. 4. Pore pressure in the nucleus pulposus centre and the posterior region of annulus
(the initial permeability of k = 1.0 e-13 m^4/Ns, k = 7.0 e-15 m^4/Ns, k = 1.0 e-48 m^4/Ns, respectively)

After 4 hours loading, the fluid loss amount of IVD is 13.8%, 13% and 12.6%, respectively, according to the 3 different permeability parameters of endplates. During the unloading phase, the model with larger permeability recovers fast, although the fluid loss increases in Fig. 2. During the three resting time periods, the fluid recovery of the model with permeability of 1.0e-13 m^4/Ns is larger than other cases by 0.4% and 1%. According to the 3 permeability parameters, after 4 hours loading, the increments of radial strain at the posterior region of annulus fibrosus are 17.4%, 16.7% and 15.5%, respectively, as shown in Fig. 3.

The pore pressure variation in nucleus pulposus and annulus fibrosus is shown in Fig. 4. The pore pressure of nucleus pulposus decreases to 0.52 MPa, 0.48 MPa and 0.448 MPa after 4 hours according to the three permeability parameters. The pore pressure of annulus fibrous decreases to 0.22 MPa, 0.21 MPa and 0.185 MPa after 4 hours. Figure 5 shows the pore pressure of annulus fibrosus and nucleus pulposus for

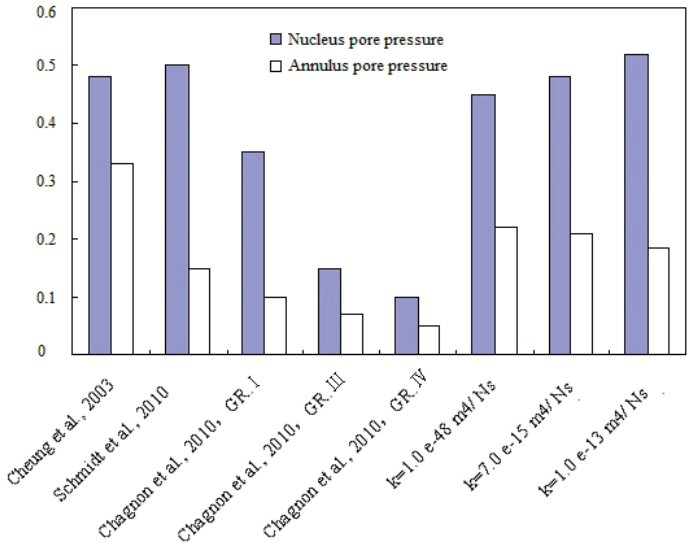

Fig. 5. Comparison of the pore pressure of intervertebral disc with the vivo studies for three FE models

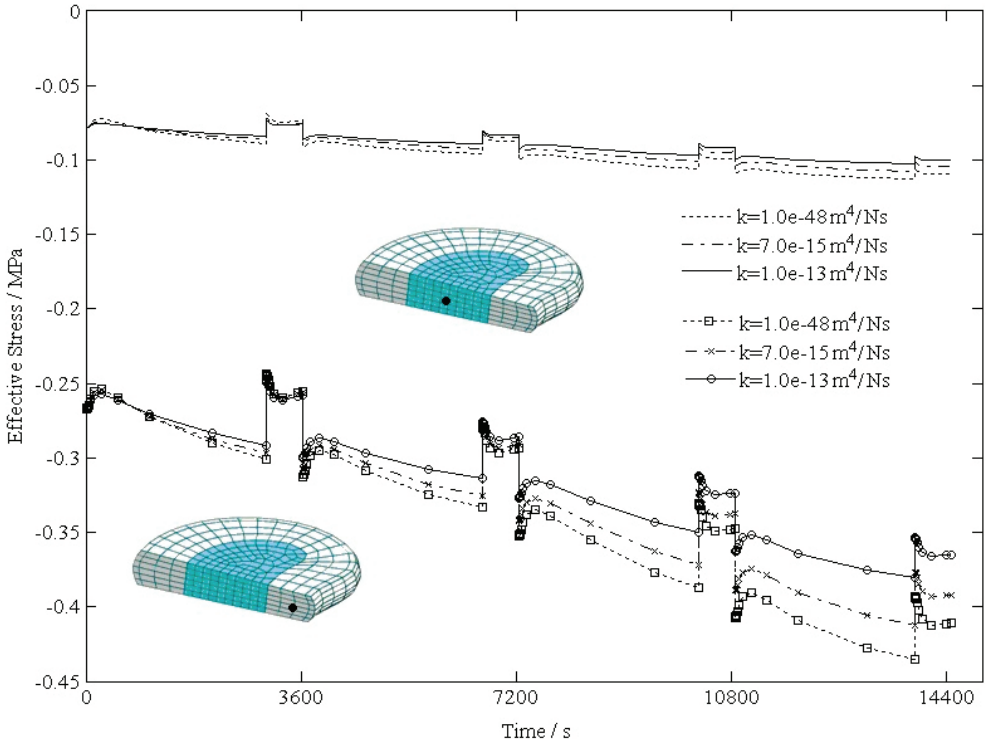

Fig. 6. Axial effective stress in the nucleus pulposus centre and posterior region of annulus (the initial permeability of k = 1.0 e-13 m^4/ Ns, k = 7.0 e-15 m^4/ Ns, k = 1.0 e-48 m^4/ Ns, respectively)

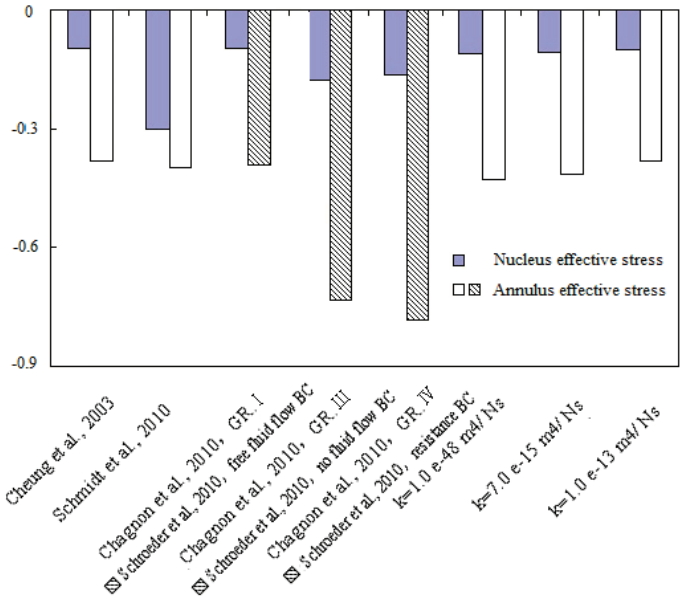

Fig. 7. Comparison of the axial effective stress with the vivo studies

different permeability of endplates (k = 1.0e-13 m^4/Ns, k = 7.0e-15 m^4/Ns, k = 1.0e-48 m^4/Ns).

The effective stress variation in nucleus pulposus and annulus fibrosus is shown in Fig. 6. The effective stress of nucleus pulposus reaches 0.1017 MPa, 0.1085 MPa and 0.11 MPa according to the 3 permeability parameters of endplates. The external effective stress of annulus fibrosus reaches 0.38 MPa, 0.415 MPa and 0.43 MPa according to the 3 permeability parameters. The compressive stress is negative as shown in Fig. 6. Figure 7 shows the effective stress of annulus fibrosus and nucleus pulposus for different permeability of endplates (k = 1.0e-13 m^4/Ns, k = 7.0e-15 m^4/Ns, k = 1.0e-48 m^4/Ns).

3.3. Condition of fluid flow

Figure 8 shows the total stress graphs at the time of 60 s, 3600 s and 14400 s, while the permeability of endplates is 7.0e-15 m^4/Ns. It can be seen that the total stress of annulus fibrosus increases with time while the total stress of nucleus pulposus decreases with time. At the initial loading step (t = 60 s), the nucleus pulposus supports most of the compressive load, but the annulus fibrosus is the main load-bearing holder after 4 hours (t = 14400 s). This phenomenon implies that a part of external load supported by nucleus pulposus gradually transfers to annulus fibrosus due to the fluid flowing in spinal components.

The pore fluid effective velocity at the initial loading and at the end of unloading is shown in Fig. 9a and Fig. 9b when the endplate permeability is 7.0e-15 m^4/Ns. The velocity vector variation in the loading step is shown in Fig. 9c, and the velocity vector variation in the unloading step is shown in Fig. 9d. It can be seen that the fluid flow velocity in the loading step is faster than the velocity in the unloading step, so this implies that a short resting time can relieve fatigue but recover to the original condition of liquid in the disc. The

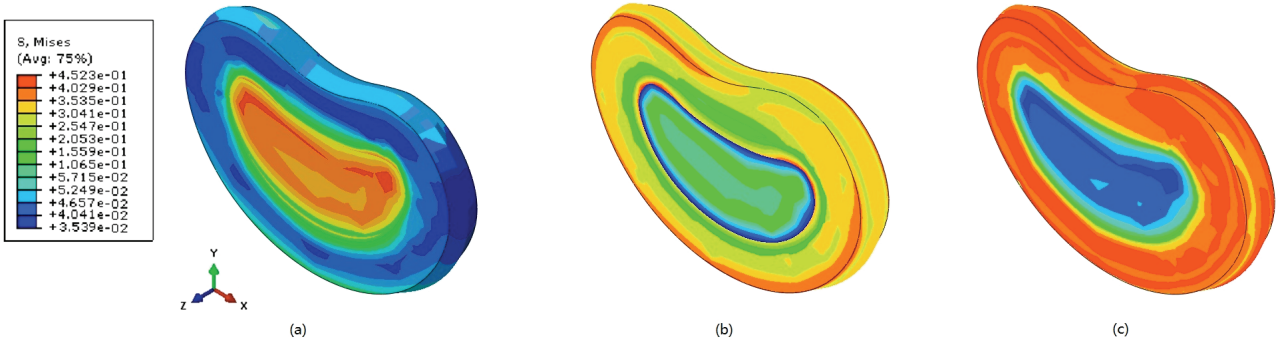

Fig. 8. The total stress of disc at the times of 60 s, 3600 s and 14400 s, respectively: (a) t = 60 s, (b) t = 3600 s, (c) t = 14400 s

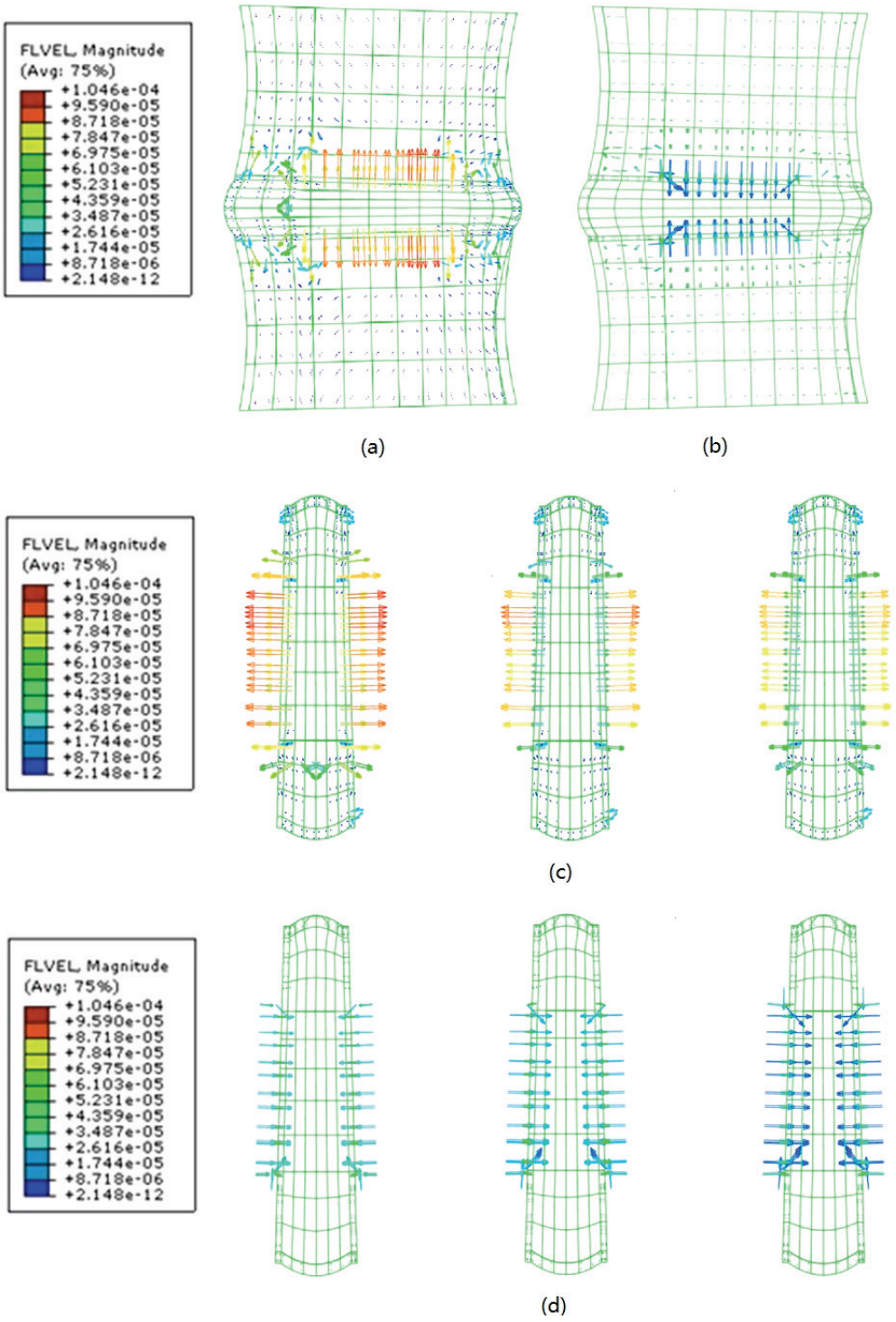

Fig. 9. Pore fluid effective velocity of the L4-L5 disc-vertebra segment at the loading step and the unloading step (the vector arrows show the fluid flowing direction): (a) the L4-L5 disc-vertebra segment at the loading step, (b) the L4-L5 disc-vertebra segment at the unloading step, (c) the disc for the three models in the loading step, (d) the disc for the three models at the unloading step

velocity vectors in Fig. 9a–d show most of the liquid in the disc flowing into vertebrae through endplates and a small quantity of liquid flowing into vertebrae through annulus fibrosus at the loading step, however, at the unloading step, almost all the liquid flowing into IVD is through endplates. In addition, the degenerated endplate (with low permeability) yields high decreasing gradient of flow velocity, which might impede the liquid inflowing or outflowing smoothly through endplates.

4. Discussion

A poroelastic FEM of L4-L5 disc-vertebra segment was established in this study and different permeability of cartilage endplates was analyzed to investigate the biomechanical response of IVD under intermittent compressive loads. Previous investigations reported that the permeability and porosity which change with strain and height of IVD are the important factors for influencing poroelastic property of IVD. However, the role of endplate permeability parameters on IVD degeneration has not been paid much attention. In this study, the endplate permeability parameters of the poroelastic FEM are assigned with different permeability values, 1.0e-13 m^4/Ns, 7.0e-15 m^4/Ns and 1.0e-48 m^4/Ns [26], [24] to study the influence of endplate permeability parameters on biomechanical characteristics of IVD under actual loading conditions. The poroelastic FEM includes L4-L5 vertebrae, IVD and two endplates without modeling the posterior elements. Compared with an integrated spinal motion segment, this simplification might be a limitation, however, it may not make much significant influence on the analytical results. In this designed loading condition, this model only suffers from the compressive load and the facets and posterior ligaments receive no force, so the simplification can meet the research aim requirements of this study. Actually, previous studies have proved the simplified modeling is reasonable [6] and the experimental result shows that in a pure axial compression, the posterior elements have little effect on IVD.

As a result of physiological function degeneration of human body, IVD degeneration usually starts in the middle-age period, along with the loss of collagen and moisture, which might cause the height of IVD to reduce and the stiffness of annulus fibrosus to increase, at the same time the stress distribution in nucleus pulposus and annulus fibrosus changes as the structure and material properties change while the disc degeneration begins to happen. Investigations showed that the failure of annulus fibrosus begins at the internal side of connection regions of endplate and annulus fibrosus. The failure might change the fluid flow pattern and nutrition channel in vertebrae and IVDs [20]. Once the inner region of annulus fibrosus fails, the load would be mainly transferred to the external region of annulus fibrosus, as a result, higher stress occurs in the external region of annulus fibrosus. Figure 8 shows that the stress distribution of each part of IVD changes with time.

Investigations have shown that swelling stress of IVD caused by fixed charge density (FCD) of proteoglycan and the permeability changing with strain plays an important role on biomechanical characteristics of IVD. The FCD of proteoglycan prevents deformation of tissue by strengthening organization function; while the permeability changing with strain limits the rate of stress transferring from liquid phase to solid phase [14]. The FCD of proteoglycan has the role of impeding fluid flowing out of the disc, which may affect the water content of tissue [27].

The swelling pressure caused by proteoglycan is the motive power of fluid flowing into IVD from surrounding tissue and the resistance of fluid flowing out of IVD. The change of velocity vector of fluid in the loading and unloading process can be seen in Fig. 9. The decrease of flow velocity with time passing by during the loading process is caused by the pore density which decreases with strain, and the decrease of flow velocity with time during the unloading process is caused by the pressure gradient which also decreases with time.

Permeability parameter values are set as 1.0e-13 m^4/Ns, 7.0e-15 m^4/Ns and 1.0e-48 m^4/Ns, respectively. The stress variation rate of nucleus pulposus and annulus fibrosus will be more moderate due to the permeability parameters decreasing. This permeability variation is similar to different degenerative levels of IVD, i.e., GRI, GRIII, GRIV [6]. The stress variation of the healthy disc GRI is obviously smaller than theose of the degenerated disc GRIII and GRIV. This indicates that the permeability of cartilage endplate is one of the factors that can be used to evaluate the degeneration of IVD.

5. Conclusions

A poroelastic FEM is established to investigate the effect of different permeability of endplates on biomechanical characteristics of spine under intermittent compression loads. The results show that the pore pressure of nucleus pulposus and annulus fibrosus of IVD decreases with time and the effective stress increases with time. The swelling pressure can form the resistance to reduce the fluid flowing out, and form the motive power to promote the fluid flowing back into tissue during unloading progress. Due to the porosity of solid tissue decreasing with time, the rate of fluid flow decreases during the loading phase. Due to the pressure gradient reducing, the rate of fluid flowing back into the tissue decreases

during the unloading process. The permeability of cartilage endplates is one of the indicators for evaluating IVD degeneration. In reasonable value range, the lower the permeability of the endplate is, the better function the disc has.

Acknowledgements

This work was supported by the National Natural Science Foundation of China (51275082, 11272273), Fundamental Research Fund of Central Universities (N130403009), Research Fund for Doctoral Program of Higher Education (20100042110013), Program for Liaoning Innovative Research Team in University (LT2014006) and Open Foundation of Key Discipline of Mechanical Design and Theory of Shenyang Ligong University (4771004kfx08).

References

[1] ADAMS M.A., MCMILLAN D.W., GREEN T.P., DOLAN P., *Sustained loading generates stress concentrations in lumbar intervertebral discs*, Spine (Phila Pa 1976), 1996, Vol. 21, 434–438.

[2] ALDRIDGE J.S., RECKWERDT P.J., MACKIE T.R., *A proposal for a standard electronic anthropomorphic phantom for radiotherapy*, Med. Phys., 1999, Vol. 26(9), 1901–1903.

[3] ARGOUBI M., SHIRAZI-ADL A., *Poroelastic creep response analysis of a lumbar motion segment in compression*, J. Biomech., 1996, Vol. 29, 1331– 1339.

[4] AYOTTE D.C., ITO K., TEPIC S., *Direction-dependent resistance to flow in the endplate of the intervertebral disc: an ex vivo study*, J. Orthop. Res., 2001, Vol. 19, 1073–1077.

[5] BORKOWSKI P., MAREK P., KRZESINSKI G., RYSZKOWSKA J., WASNIEWSKI B., WYMYSLOWSKI P., ZAGRAJEK T., *Finite element analysis of artificial disc with an elastomeric core in the lumbar spine*, Acta of Bioengineering and Biomechanics, 2012, Vol. 14(1), 59–66.

[6] CHAGNON A., AUBIN C.E., VILLEMURE I., *Biomechanical Influence of Disk Properties on the Load Transfer of Healthy and Degenerated Disks Using a Poroelastic Finite Element Model*, ASME Journal of Biomechanical Engineering, 2010, Vol. 132(11), No. 1111006-1-7

[7] CHEUNG J.T.M., ZHANG M., CHOW D.H.K., *Biomechanical responses of the intervertebral joints to static and vibrational loading: a finite element study*, Clinical Biomechanics, 2003, Vol. 18, 790–799.

[8] FERGUSON S.J., ITO K., NOLTE L.P., *Fluid flow and convective transport of solutes within the intervertebral disc*, J. Biomech., 2004, Vol. 37(2), 213–221.

[9] FROBIN W., BRINCKMANN P., BIGGEMANN M., TILLOTSON M., BURTON K., *Precision measurement of disc height, vertebral height and sagittal plane displacement from lateral radiographic views of the lumbar spine*, Clin. Biomech. (Bristol, Avon), 1997, Vol. 12, 1–63.

[10] GOHARI E., NIKKHOO M., HAGHPANAHI M., PARNIANPOUR M., *Analysis of different material theories used in a FE model of a lumbar segment motion*, Acta of Bioengineering and Biomechanics, 2013, Vol. 15(2), 33–41.

[11] GU W.Y., MAO X.G., FOSTER R.J. et al., *The anisotropic hydraulic permeability of human lumbar annulus fibrosus. Influence of age, degeneration, direction, and water content*, Spine, 1999, Vol. 24(23), 2449–2455.

[12] GUO L.X., ZHANG M., TEO E.C., *Influences of denucleation on contact force of facet joints under whole body vibration*, Ergonomics, 2007, Vol. 50(7), 967–978.

[13] GUO L.X., ZHANG Y.M., ZHANG M., *Finite element modeling and modal analysis of the human spine vibration configuration*, IEEE Transactions on Biomedical Engineering, 2011, Vol. 58(10), 2987–2990.

[14] HUSSAINA M., NATARAJAN R.N., CHAUDHARYD G., AN H.S., ANDERSSON G.B.J., *Relative contributions of strain-dependent permeability and fixed charged density of proteoglycans in predicting cervical disc biomechanics: A poroelastic C5-C6 finite element model study*. Medical Engineering & Physics, 2011, Vol. 33, 438–445.

[15] JARAMILLO H.E., GOMEZ L., GARCIA J.J., *A finite element model of the L4-L5-S1 human spine segment including the heterogeneity and anisotropy of the discs*, Acta of Bioengineering and Biomechanics, 2015, Vol. 17(2), 15–24.

[16] LEE K.K., TEO E.C., *Poroelastic analysis of lumbar spinal stability in combined compression and anterior shear*, Journal of Spinal Disorders & Techniques, 2004, Vol. 17(5), 429–438.

[17] LU Y.M., HUTTON W.C., GHARPURAY V.M., *Do bending, twisting, and diurnal fluid changes in the disc affect the propensity to prolapse? A viscoelastic finite element model*, Spine, 1996, Vol. 21(22), 2570–2579.

[18] MACLEAN J.J., OWEN J.P., IATRIDIS J.C., *Role of endplates in contributing to compression behaviors of motion segments and intervertebral discs*, J Biomech, 2007, Vol. 40, 55–63.

[19] MROZ A., SKALSKI K., WALCZYK W., *New lumbar disc endoprosthesis applied to the patient's anatomic features*, Acta of Bioengineering and Biomechanics, 2015, Vol. 17(2), 25–34.

[20] NATARAJAN R.N., WILLIAMS J.R., LAVENDER S.A., ANDERSSON G.B.J., *Poro-elastic finite element model to predict the failure progression in a lumbar disc due to cyclic loading*, Computers and Structures, 2007, Vol. 85, 1142–1151.

[21] PAWLIKOWSKI M., SKALSKI K., SOWINSKI T., *Hyper-elastic modelling of intervertebral disc polyurethane implant*, Acta of Bioengineering and Biomechanics, 2013, Vol. 15(2), 43–50.

[22] PRZYBYLA A., POLLINTINE P., BEDZINSKI R., *Outer annulus tears have less effect than endplate fracture on stress distributions inside intervertebral discs: Relevance to disc degeneration*, Clinical Biomechanics, 2006, Vol. 21(10), 1013–1019.

[23] SCHMIDT H., SHIRAZI-ADL A., GALBUSERA F., WILKE H.J., *Response analysis of the lumbar spine during regular daily activities – A finite element analysis*, Journal of Biomechanics, 2010, Vol. 43, 1849–1856.

[24] SCHROEDER Y., HUYGHE J.M., VAN DONKELAAR C.C., ITO K., *A biochemical/biophysical 3D FE intervertebral disc model*, Biomech. Model. Mechanobiol. 2010, Vol. 9, 641–650.

[25] SHIRAZI-ADL A., PARNIANPOUR M., *Load-bearing and stress analysis of the human spine under a novel wrapping compression loading*, Clinical Biomechanics (Bristol, Avon), 2000, Vol. 15(10), 718–725.

[26] SMITH L.J., FAZZALARI N.L., *The Elastic Fibre Network of the Human Lumbar Anulus Fibrosus: Architecture, Mechanical Function and Potential Role in the Progression of Intervertebral Disc Degeneration*, European Spine Journal, 2009, Vol. 18(4), 439–448.

[27] URBAN J.P., MCMULLIN J.F., *Swelling pressure of the lumbar intervertebral discs: influence of age, spinal level, composition, and degeneration*, Spine, 1988, Vol. 13, 179–87.

[28] VAN DER VEEN A.J., MULLENDER M., SMIT T.H., KINGMA I., DIEEN J.H., *Flow-related mechanics of the intervertebral disc: the validity of an in vitro model*, Spine, 2005, Vol. 30(18), E534–539.

[29] WILKE H.J., NEEF P., CAIMI M., HOOGLAND T., CLAES L.E., *New in vivo measurements of pressures in the intervertebral disc in daily life*, Spine, 1999, Vol. 24(8), 755–762.

[30] WU J.S.S., CHEN J.H., *Clarification of the mechanical behavior of spinal motion segments through a three-dimensional poroelastic mixed finite element model*, Med. Eng. Phys., 1996, Vol. 18(3), 215–244.